Available online at www.sciencedirect.com
SCIENCE DIRECT®
Biochemical and Biophysical Research Communications 307 (2003) 172–179
BBRC
www.elsevier.com/locate/ybbrc

Specificity for inhibitors of metal-substituted methionine aminopeptidase☆,☆☆

Jing-Ya Li,[a] Ling-Ling Chen,[a] Yong-Mei Cui,[a] Qun-Li Luo,[a] Jia Li,[a] Fa-Jun Nan,[a,*] and Qi-Zhuang Ye[a,b,*]

[a] *Chinese National Center for Drug Screening, Shanghai Institute of Materia Medica, Shanghai Institutes for Biological Sciences, Chinese Academy of Sciences, 189 Guo-Shou-Jing Road, Shanghai 201203, China*
[b] *The High Throughput Screening Laboratory, Higuchi Biosciences Center, University of Kansas, 1501 Wakarusa Dr., Lawrence, KS 66047-1803, USA*

Received 2 June 2003

Abstract

Methionine aminopeptidases (MetAPs) have been studied in vitro as Co(II) enzymes, but their in vivo metal remains to be defined. While activation of *Escherichia coli* MetAP (*Ec*MetAP1) by Co(II), Mn(II), and Zn(II) was detectable by a colorimetric Met–*S*–Gly–Phe assay, significant activation by Ni(II) was shown in a fluorescence Met-AMC assay, in addition to Co(II) and Mn(II) activation. When tested on the metal-substituted *Ec*MetAP1s, a few inhibitors that we obtained recently from a random screening on Co-*Ec*MetAP1 either became much weak or lost activity on Mn- or Zn-*Ec*MetAP1, although they kept inhibitory activity on Ni-*Ec*MetAP1. A couple of peptidic inhibitors and the methionine mimetic (3*R*)-amino-(2*S*)-hydroxyheptanoic acid (AHHpA, **6**) maintained moderate activities on Co-, Mn-, Zn-, and Ni-*Ec*MetAP1s. Our results clearly demonstrate that the metal-substitution has changed the enzyme specificity for substrates and inhibitors. Therapeutic applications call for inhibitors specific for MetAP with a physiologically relevant metal at its active site.

Methionine aminopeptidase (MetAP) carries out the important function of removing the initiator methionine residue from nascent proteins [1,2]. Prokaryotes have only one MetAP, while eukaryotic cells contain both type I and type II MetAPs. Eubacteria (*Escherichia coli*, *Bacillus subtilis*, and *Salmonella typhimurium*) have only type I MetAPs, and archaea (*Methanobacterium thermoautotrophicum*, *Sulfolobus solfataricus*, and *Pyrococcus furiosis*) have only type II MetAPs. Although the enterohaemorrhagic *E. coli* strain O157:H7 has more than 20% of 5416 genes different from the *E. coli* laboratory strain K-12 [3], it has exactly the same MetAP sequence. Deletion of the MetAP gene from *E. coli* [4] or *S. typhimurium* [5] was lethal, demonstrating the essential role of the MetAP enzymes in bacteria. Deletion of either type I or type II MetAP from the yeast *Saccharomyces cerevisiae* rendered a slow growth phenotype, and removal of both the MetAPs made the yeast nonviable [6]. Therefore, MetAPs are the potential targets for developing antibacterial and antifungal drugs [7]. Although the antiangiogenic mechanism of natural product fumagillin and its analogues, such as TNP-470 in clinical trials for cancer, has not been fully understood, they are potent inhibitors of type II MetAP in human and covalently modified the enzyme [8,9], indicating the possible involvement of MetAPs in cancer angiogenesis.

☆ This research has been supported by the National Natural Science Foundation of China Grants 30271528 (F.-J.N.) and 39725032 (Q.-Z.Y.) and by the NIH COBRE award 1 P20 RR15563 and matching support from the State of Kansas (Q.-Z.Y.).

☆☆ *Abbreviations:* MetAP, methionine aminopeptidase; *Ec*MetAP1, *E. coli* MetAP type I; HTS, high-throughput screening; DTNB, 5,5′-dithiobis(2-nitrobenzoic acid); AMC, 7-amido-4-methylcoumarin; AHHpA, (3*R*)-amino-(2*S*)-hydroxyheptanoic acid; GSH, reduced glutathione; BSA, bovine serum albumin.

* Corresponding authors. Fax: 1-785-330-4332 (Q.-Z. Ye) or +86-21-5080-0721 (F.-J. Nan).

E-mail addresses: qye@ku.edu (Q.-Z. Ye), fjnan@mail.shcnc.ac.cn (F.-J. Nan).

0006-291X/03/$ - see front matter © 2003 Elsevier Science (USA). All rights reserved.
doi:10.1016/S0006-291X(03)01144-6

MetAPs have been studied in vitro as Co(II) enzymes with a dinuclear active site, as seen in several available X-ray structures [10–12]. Like many other metalloenzymes, MetAPs could be reproducibly activated by Co(II) and considered as a Co(II) enzyme because of the high activity in the presence of Co(II) when compared to the activity levels of other divalent metal ions. However, Walker and Bradshaw [13] questioned the metal identity when they observed that in the presence of physiological concentration of reduced glutathione (GSH), the activity of Zn(II) substituted type I MetAP from *S. cerevisiae* (*Sc*MetAP1) was increased 1.7-fold, while Co(II) substitution became inactive, suggesting Zn(II) as a possible in vivo metal. Yang et al. [14], however, found that type II MetAP from human (*Hs*MetAP2) could not be activated by Zn(II) and attributed the stoichiometric amount of Zn(II) during purification to a binding external to the active site. It has been suggested that the in vivo metal ion for the MetAP from *E. coli* (*Ec*MetAP1) is Fe(II) on the basis of a combination of whole cell metal analyses and activity measurements under anaerobic condition [15]. In addition, the observed catalytic activity related to the amount of divalent metal ion and the metal binding constants for both Fe(II) and Co(II) to *Ec*MetAP1 led to the proposal that *Ec*MetAP1 functions as a mononuclear Fe(II) enzyme in vivo [16]. The high-affinity or catalytically relevant metal binding site was assigned as the histidine-containing site according to an NMR experiment which observed the His-171 signal. More recently, the MetAP from *Pyrococcus furiosis* (*Pf*MetAP2), a type II enzyme, was also characterized for metal requirements, and like *Ec*MetAP1, maximum catalytic activity was obtained with one equivalent of Co(II) or Fe(II) [17].

Since the importance of MetAPs in bacterial and fungal life cycle and the potential involvement of *Hs*MetAP2 in angiogenesis, there are intensive efforts in developing MetAP inhibitors, usually using the Co(II)-substituted MetAPs. However, uncertainty of the in vivo metal casts doubts on whether these Co-MetAP inhibitors would be effective in vivo against the MetAPs in their native states with a metal other than Co(II) at their active site. In our report, we prepared an apo-enzyme of *Ec*MetAP1 and characterized the metal-substituted *Ec*MetAP1s for hydrolysis of synthetic substrates and inhibition by novel inhibitors obtained from random screening. The information presented here suggests that MetAP inhibitors with specificity for MetAP with a physiologically relevant metal are required for clinical success.

Materials and methods

Materials and instruments. Chromogenic thiopeptolide substrate Met–*S*–Gly–Phe was synthesized in this laboratory according to a literature procedure [18]. Fluorogenic substrate Met-AMC was from Bacham Bioscience (King of Prussia, PA). Expression vector pGEMEX-1 and restriction enzymes were purchased from Promega (Madison, WI). The 5260 compounds used for random screening were all small organic compounds with unrelated and diverse chemical structures and purchased from SPECS/BioSPECS (Rijswijk, The Netherlands) with purity higher than 90%.

Continuous kinetic monitoring of enzyme activity was performed on either SpectraMax 340 microplate reader for UV absorption or fmax microplate reader for fluorescence, both were from Molecular Devices (Sunnyvale, CA) and controlled by the Softmax software. Liquid handling for random screening was carried out on the ORCA automation system with a Biomek 2000 liquid handling workstation from Beckman Coulter (Fullerton, CA) and with the Hydro 96 semi-automated 96-channel pipettor from Robins (Sunnyvale, CA). Protein purification was carried out on an AKTA FPLC system with UV and conductivity monitors (Amersham Biosciences, Piscataway, NJ).

Preparation of apo-EcMetAP1. The full-length gene of *Ec*MetAP1 was obtained by direct PCR-amplification from an *E. coli* strain BL21(DE3)pLysS with introduction of restriction sites for *Nhe*I and *Eco*RI. The PCR primers had the following sequences: forward, GGTT*GCTAGC*TCAATCAAGACCCCAGAA and reverse, GCACC *GAATTC*TTATTCGTCGTGCGAGAT (the restriction sites are in italics and the coding sequences underlined). The PCR fragment was cloned into the vector pGEMEX-1 and the recombinant plasmid was transformed into the BL21(DE3)pLysS strain for expression.

The *E. coli* strain containing the *Ec*MetAP1 expressing plasmid was cultured in 500 mL LB media at 37 °C, and when OD reached 0.6, the expression of recombinant *Ec*MetAP1 was induced by adding IPTG to 0.5 mM and allowed to continue for 5 h at 30 °C. Cells (0.8 g cell paste) from the 500 mL culture were resuspended in 15 mL buffer A (50 mM Hepes, pH 7.5, 150 mM KCl, 15 mM methionine, and 5 mM EDTA) with 0.1% Triton X-100 and sonicated for 2 min on ice. After centrifugation at 12,000*g* for 15 min, solid $(NH_4)_2SO_4$ was added to the supernatant to 60% saturation. The mixture was centrifuged again and the clarified supernatant was loaded onto a 55 mL HiPrep desalting column previously equilibrated with the buffer A, to remove $(NH_4)_2SO_4$. The active protein fractions were then loaded onto a 5 mL HiPrep Q–Sepharose column equilibrated with the buffer A, and the active protein was in the flowthrough fractions. The protein was exchanged into 50 mM Hepes, pH 7.5, with 150 mM KCl with a desalting column and dialyzed against the Hepes buffer for 72 h. The purified apo-*Ec*MetAP1 protein (20 mg) showed a singe band on SDS–PAGE gel by Coomassie blue staining.

Protein concentration determination and metal analysis. Protein concentration was determined by the BCA protein assay with a kit from PIERCE (Rockford, IL) with bovine serum albumin (BSA) as the protein standard. The protein concentration was further calibrated by a DTNB titration, taking advantage of the known number of cysteines in the purified apo-*Ec*MetAP1. In the DTNB titration, the absorbance at 412 nm was measured when the apo-*Ec*MetAP1 (<50 μM) was mixed in 50 mM Mops, pH 7.0, 6 M guanidine hydrochloride, and 2 mM DTNB, and the amount of protein was calculated from a standard curve obtained using known amounts of L-cysteine. Metal analysis of the apo-*Ec*MetAP1 solution was carried out by inductively coupled plasma-atomic emission spectrometry (ICP-AES) method. The Co, Fe, Mn, Ni, and Zn were <0.004, 0.005, <0.002, <0.002, and 0.004 ppm, respectively, and none of them was above 0.1 μM for the 1.0 μM protein solution.

EcMetAP1 activity assays. Chromogenic assays using the thiopeptolide Met–*S*–Gly–Phe were carried out as described [18] with modifications for reading on microplates and for high-throughput screening (HTS). The assay was usually performed at room temperature on a 96-well clear polystyrene microplate. In metal activation experiments, the assay mixture in each well contained 50 mM Mops, pH 7.0, 1 mM DTNB, 100 μM Met–*S*–Gly–Phe, 1.0 μM apo-*Ec*MetAP1, and various amounts of metal ion ($CoCl_2$, $MnCl_2$, $ZnCl_2$, or $NiCl_2$). The hydrolysis of Met–*S*–Gly–Phe was monitored continuously by change of UV absorbance at 412 nm, and the initial rate of the

hydrolysis was determined using the early linear region of the enzymatic reaction curve. The rate for background hydrolysis of the thiopeptolide was subtracted.

Assays with the fluorogenic substrate Met-AMC were also performed on 96-well clear polystyrene microplates. The formation of 7-amido-4-methylcoumarin (AMC) was monitored continuously for usually 30 min at room temperature by fluorescence ($\lambda_{ex} = 360$ nm, $\lambda_{em} = 460$ nm). In the metal activation experiments, each 100 μL assay mixture contained 50 mM Mops, pH 7.0, 400 μM Met-AMC, 1.0 μM apo-*Ec*MetAP1, and various amounts of metal ion ($CoCl_2$, $MnCl_2$, $ZnCl_2$, or $NiCl_2$).

EcMetAP1 inhibitor screening. A library of 5260 pure organic compounds was screened against recombinant Co-*Ec*MetAP1 using Met–*S*–Gly–Phe as the substrate. Immediately before the assay, the apo-*Ec*MetAP1 was preincubated for 30 min in a mixture with 1.5 μM apo-*Ec*MetAP1, 500 μM $CoCl_2$, 50 mM Hepes, pH 7.5, 150 mM KCl, and 15 mM methionine. The enzymatic assay was carried out on 96-well clear polystyrene plates in a 100 μL volume in each well containing 50 mM Mops, pH 7.0, 1 mM DTNB, 100 μM Met–*S*–Gly–Phe, 10 μL of the Co(II) activated *Ec*MetAP1 (final concentrations: 150 nM *Ec*MetAP1, 50 μM $CoCl_2$), 20 μg/mL compound, and 2% DMSO. The hydrolysis of Met–*S*–Gly–Phe was monitored on SpectraMax 340 microplate reader at 412 nm for 1 min at room temperature.

Kinetic characterization of metal-substituted EcMetAP1s and their inhibitors. We characterized the metal-substituted *Ec*MetAP1s by determining their kinetic parameters k_{cat}, K_m, and k_{cat}/K_m values for substrates and K_i values for inhibitors using either the chromogenic Met–*S*–Gly–Phe or the fluorogenic Met-AMC.

To obtain the k_{cat}, K_m, k_{cat}/K_m, and K_i values using Met–*S*–Gly–Phe, a 100 μL assay mixture contained 50 mM Mops, pH 7.0, 1 mM DTNB, 100 nM apo-*Ec*MetAP1, 10 μM $CoCl_2$, and Met–*S*–Gly–Phe in twofold dilutions up to 5 mM with or without an inhibitor. The k_{cat} and K_m values of the metal-substituted *Ec*MetAP1 in the presence and absence of the inhibitor were derived from a non-linear regression fitting of the curve in the plot of the initial rates vs. the substrate concentrations, using the Michaelis–Menton equation $v = V_{max} \cdot [S]/(K_m + [S])$. In the presence of competitive inhibitors, the equation is described as $1/v = [K_m/(V_{max} \cdot [S])](1 + [I]/K_i) + 1/V_{max}$. K_i values were obtained by the linear re-plot of apparent K_m/V_{max} (slope) from primary reciprocal plot vs. inhibitor concentration [I] according to the equation $K_m/V_{max} = 1 + [I]/K_i$.

In determining k_{cat} and K_m values using the fluorogenic Met-AMC, a 100 μL assay mixture contained 50 mM Mops, pH 7.0, 1 μM apo-*Ec*MetAP1, 100 μM $CoCl_2$, and Met-AMC in twofold dilutions up to 10 mM. Since the presence of Met-AMC at high concentration affects the fluorescence of AMC, standard curves for the fluorescence of AMC in the presence of the specific amounts of Met-AMC were generated and used for calculating the rate of Met-AMC hydrolysis or the rate of AMC formation, assuming that the amount of Met-AMC did not change significantly during the initial rate determination. The k_{cat} and K_m values were obtained by non-linear curve fitting of the Michaelis–Menten equation.

The IC_{50} is the compound concentration at which 50% of the enzyme activity is inhibited and was obtained from the non-linear curve fitting of percent inhibition (% inhibition) vs. inhibitor concentration [I] by using the equation, $\%\text{inhibition} = 100/\{1 + (IC_{50}/[I])^k\}$, where k is the Hill coefficient.

Results

Preparation of apo-EcMetAP1

Overexpression of *Ec*MetAP1 in *E. coli* was achieved by cloning the *Ec*MetAP1 gene into pGEMEX-1 for an IPTG-inducible expression under the control of a T7 promoter. *Ec*MetAP1 was expressed as a soluble protein and purified by precipitation with $(NH_4)_2SO_4$ and ion-exchange chromatography. We have purified the apo-enzyme with EDTA included early in the cell lysis buffer or with adding EDTA at the very last buffer exchange step, and they worked equally well. When the protein was purified without adding divalent metal ions and removing adventurous metals in the buffer, the purified protein showed a basal activity. However, this basal activity could be effectively reduced to an undetectable level by EDTA treatment. Our apo-*Ec*MetAP1 preparation showed no detectable activity and could be reproducibly activated by Co(II). The yield was usually 20 mg of apo-*Ec*MetAP1 from a 500 mL culture and the purified protein showed a single band on the SDS–PAGE gel. Metal analysis showed no significant amount of Co, Fe, Mn, Ni, or Zn in the protein preparation.

Activation of EcMetAP1 by divalent metal ions

Using the continuous assays with synthetic chromogenic and fluorogenic substrates, we tested activation of the apo-*Ec*MetAP1 by different divalent metal ions.

With the chromogenic Met–*S*–Gly–Phe as the substrate [18], activity of *Ec*MetAP1 increased along with increasing amounts of $CoCl_2$ until $CoCl_2$ concentration was approaching one equivalent of the apo-*Ec*MetAP1, which was 1.0 μM (Fig. 1A). At concentrations above 100 μM, $CoCl_2$ started to show inhibition. The apo-*Ec*MetAP1 could also be activated by Mn(II) with activity approaching maximum at one equivalent of apo-*Ec*MetAP1. Zn(II) activation was only observed in a very narrow range close to one equivalent of apo-*Ec*MetAP1, and the strong inhibition by Zn(II) at high

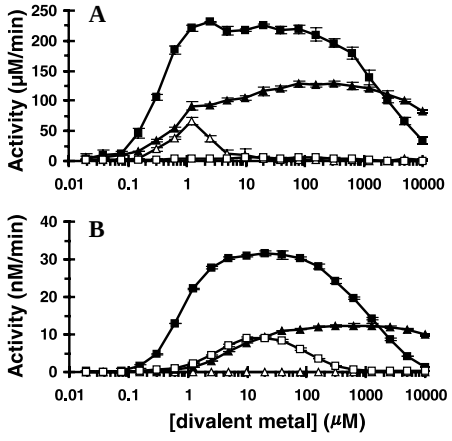

Fig. 1. Activation of apo-*Ec*MetAP1 by a divalent metal: Co(II) (filled squares), Mn(II) (filled triangles), Zn(II) (open triangles), and Ni(II) (open squares). The enzyme activity was monitored either by the hydrolysis of Met–*S*–Gly–Phe in a continuous colorimetric assay with 1.0 μM apo-*Ec*MetAP1 (A) or the hydrolysis of Met-AMC in a continuous fluorescence assay with 1.0 μM apo-*Ec*MetAP1 (B).

concentrations was observed and is currently under investigation in the laboratory. We also observed weak activation by Ni(II) and Cd(II) but no activation by Mg(II), Ca(II), or Cu(II).

Our testing of the fluorogenic Met-AMC on *Ec*MetAP1 was encouraged by the finding of Yang et al. [14] that *Hs*MetAP2 could hydrolyze Met-AMC. We found that activated apo-*Ec*MetAP1 could also cleave the amide bond in the molecule to release AMC, which can be conveniently monitored in a fluorescence assay. We carried out similar metal substitution experiments and investigated the metal activation with the substrate Met-AMC. To our surprise, we observed significant activation of apo-*Ec*MetAP1 by Ni(II), in addition to activation by Co(II) and Mn(II), but activation by Zn(II) was no longer detectable (Fig. 1B). Again, Co(II) showed inhibition at high concentration, so did Ni(II).

Preincubation of metal ion with EcMetAP1

Several MetAP assays require preincubation of apoenzyme with divalent metals [15,18]. We carried out our inhibitor screening using the continuous Met–*S*–Gly–Phe assay with a preincubation step. However, we later found no difference in enzyme activity between no preincubation and with 15 or 30 min preincubation, and the preincubation step was not necessary for the Met–*S*–Gly–Phe assay. Therefore, we carried out our Met–*S*–Gly–Phe assays, as well as the Met-AMC assays, described herein without preincubation unless specified.

Stability of EcMetAP1s

The fluorescence assay using Met-AMC is simple in assay composition with only enzyme, substrate, and buffer present, and we observed linear progression curves up to 10 h for the hydrolysis of Met-AMC by *Ec*MetAP1 with Co(II), Mn(II), or Ni(II) substitution, when sufficient amount of Met-AMC was present, indicating the stability of the metal-substituted *Ec*MetAP1s under the assay condition. On the other hand, there was a significant curvature of the progression curve during the Met–*S*–Gly–Phe assay even within one minute, and since DTNB was required in the assay mixture, we attributed it to the DTNB inactivation rather than the instability of the enzyme, which we will report in detail elsewhere.

Kinetic properties of the metal-substituted EcMetAP1s

Since we observed the activation of apo-*Ec*MetAP1 by Co(II), Mn(II), Zn(II), and Ni(II), we carried out detailed kinetic analysis in hydrolyzing Met–*S*–Gly–Phe and Met-AMC and determined the kinetic constants for the metal-substituted enzymes (Table 1). Under our assay condition, Co-*Ec*MetAP1 was an efficient enzyme in cleaving Met–*S*–Gly–Phe (k_{cat}/K_m, 23,430 $M^{-1} s^{-1}$), and Mn-*Ec*MetAP1 showed a catalytically competent enzyme with about 50% of Co(II)-*Ec*MetAP1 activity (k_{cat}/K_m, 10,917 $M^{-1} s^{-1}$). Ni-*Ec*MetAP1 is a very poor enzyme in hydrolyzing the thiopeptolide and its activity was barely detectable. However, activity of Ni-*Ec*MetAP1 could be easily detected in cleaving the fluorogenic substrate Met-AMC (k_{cat}/K_m, 1.32 $M^{-1} s^{-1}$).

Discovery of novel EcMetAP1 inhibitors

With Co-*Ec*MetAP1, we carried out a random screening of a small organic compound library for enzyme inhibitors. The 5260 compounds were initially screened at a single concentration of 20 μg/mL using the continuous assay with the chromogenic substrate Met–*S*–Gly–Phe. Several hits were identified in the screening (compounds **1**, **2**, **3**, and **4**, Fig. 2), and their inhibitory activities were confirmed by determining their IC_{50}s at multiple concentrations. We have subsequently carried out structural modifications and structure–function analyses on these lead compounds and improved inhibitory potencies [19] (IC_{50} from 1.3 μM for compound **1** to 100 nM for compound **5**, for example).

Compound **1** is among the leads we identified and it inhibited Co-*Ec*MetAP1 with characteristics typical of a competitive inhibitor, as indicated by an increased K_m

Table 1
Kinetic constants for the metal-substituted *Ec*MetAP1s

	K_m (mM)	k_{cat} (s^{-1})	k_{cat}/K_m ($M^{-1} s^{-1}$)
With Met–S–Gly–Phe[a]			
Co-*Ec*MetAP1	0.86 ± 0.03	20.2 ± 0.7	23,430
Mn-*Ec*MetAP1	3.89 ± 0.51	42.5 ± 4.4	10,917
Zn-*Ec*MetAP1	2.01 ± 0.33	11.1 ± 1.3	5513
With Met-AMC[b]			
Co-*Ec*MetAP1	4.32 ± 0.49	0.01142 ± 0.00073	2.64
Mn-*Ec*MetAP1	6.27 ± 1.24	0.00590 ± 0.00083	0.94
Ni-*Ec*MetAP1	1.24 ± 0.07	0.00164 ± 0.00008	1.32

[a] Assays with Met–*S*–Gly–Phe were carried out with 100 nM apo-*Ec*MetAP1 and 10 μM $CoCl_2$, 10 μM $MnCl_2$, or 100 nM $ZnCl_2$.
[b] Assays with Met-AMC were carried out with 1 μM apo-*Ec*MetAP1 and 100 μM $CoCl_2$, 100 μM $MnCl_2$, or 10 μM $NiCl_2$. K_m and k_{cat} values were obtained by non-linear curve fitting of the Michaelis–Menten equation.

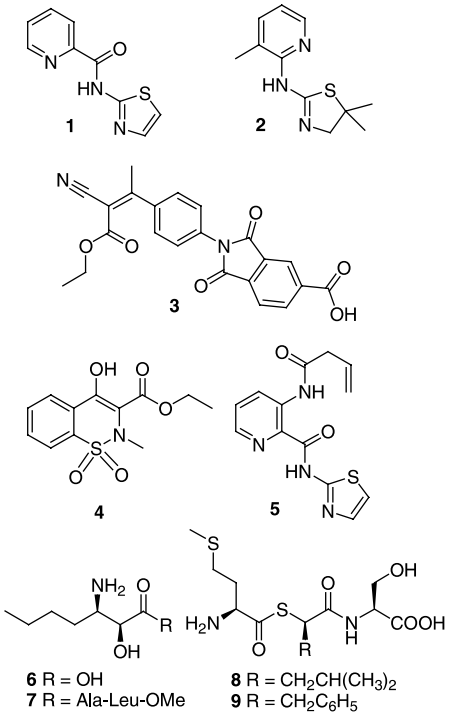

Fig. 2. Structures of *Ec*MetAP1 inhibitors.

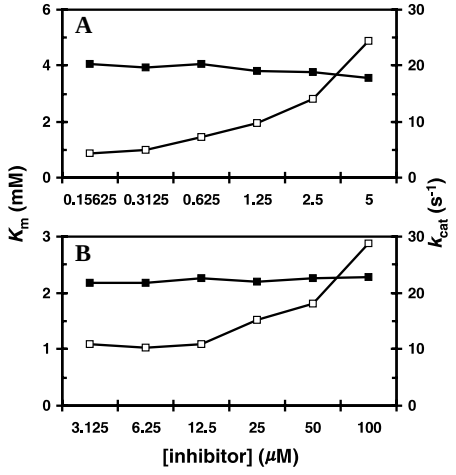

Fig. 3. Inhibition of the hydrolysis of Met–*S*–Gly–Phe by compounds **1** (A) and **6** (B). In the continuous colorimetric assays, apo-*Ec*MetAP1 was 100 nM, $CoCl_2$ was 10 μM, and Met–*S*–Gly–Phe varied from 40 μM to 5 mM. The K_m (open squares) and k_{cat} (closed squares) values were obtained by non-linear curve fitting of the Michaelis–Menten equation.

and an unchanged k_{cat} when the inhibitor concentration was increased (Fig. 3A). The calculated inhibitory constant K_i was 850 nM. Up to now, few inhibitors for any bacterial and fungal MetAPs including *Ec*MetAP1 have been reported. The substrate-like bestatin-based inhibitor AHHpA–Ala–Leu–Val–Phe–OMe had reported an IC_{50} of 5 μM [20]. Since the X-ray structure of *Ec*MetAP1 complexed with the inhibitor [10] showed only the AHHpA–Ala–Leu moiety with defined electron density, we reasoned that the AHHpA moiety itself (compound **6**) or the AHHpA–Ala–Leu–OMe fragment (compound **7**) might be an inhibitor for *Ec*MetAP1. We synthesized AHHpA and it showed a competitive inhibition pattern as compound **1** (Fig. 3B).

Change of specificity towards inhibitors upon metal substitution of EcMetAP1

We have confirmed these inhibitors on Co-*Ec*MetAP1 with normal sigmoid inhibitory curves with both substrates Met–*S*–Gly–Phe and Met-AMC (Figs. 4A and D). Since the in vivo metal may not be Co(II), it would be important to know whether inhibitors for Co-*Ec*MetAP1 will also inhibit *Ec*MetAP1 with a metal other than Co(II) at its active site. With the metal-substituted *Ec*MetAP1s available, we tested these inhibitors to find out whether they maintain their inhibitory potencies and whether there is any change in specificity for inhibitors upon metal substitution. Although AHHpA (**6**) and AHHpA–Ala–Leu–OMe (**7**) maintained similar moderate inhibitory potencies on the metal-substituted *Ec*MetAP1s tested, the inhibitors **1**, **2**, **3**, and **4** identified from random screening lost the activity on Mn- and Zn-*Ec*MetAP1s, and the improved inhibitor **5** was much weaker (Figs. 4B, C, and E, and Table 2). The two substrates (Met–*S*–Gly–Phe and Met-AMC) did not change the potency rank order, but the metal did make a difference for the inhibitory potencies. These compounds inhibited Ni-*Ec*MetAP1 with the similar potency rank order as for Co-*Ec*MetAP1 (Fig. 4F). Two thiopeptolides (compounds **8** and **9**) that we synthesized recently for a related study were not hydrolyzable by *Ec*MetAP1 because of *R* configuration at the second residue instead of *S* configuration in natural amino acids, like AHHpA, inhibited Co-, Mn-, Zn-, and Ni-*Ec*MetAP1s. Although the reasons for the differences remain to be elucidated, our results suggested that metal substitution changed the specificity for inhibitors. From our limited set of inhibitors, it seems that inhibitors behaved similarly on Co- and Ni-*Ec*MetAP1s but differently on Mn- and Zn-*Ec*MetAP1s.

Discussion

The divalent metal Co(II) is an excellent activator for several metalloenzymes including MetAPs, and all X-ray structures for MetAPs reported to date contain two Co(II) ions at the dinuclear active site [10–12]. However, some of other divalent metals have also been shown to be capable of activating the MetAP enzymes in vitro, such as Fe(II) for *Ec*MetAP1 [15,16] and *Pf*MetAP2 [17], Zn(II) for *Ec*MetAP1 [15] and *Sc*MetAP1 [13], Mn(II) for *Ec*MetAP1 [15,21] and *Sc*MetAP1 [13],

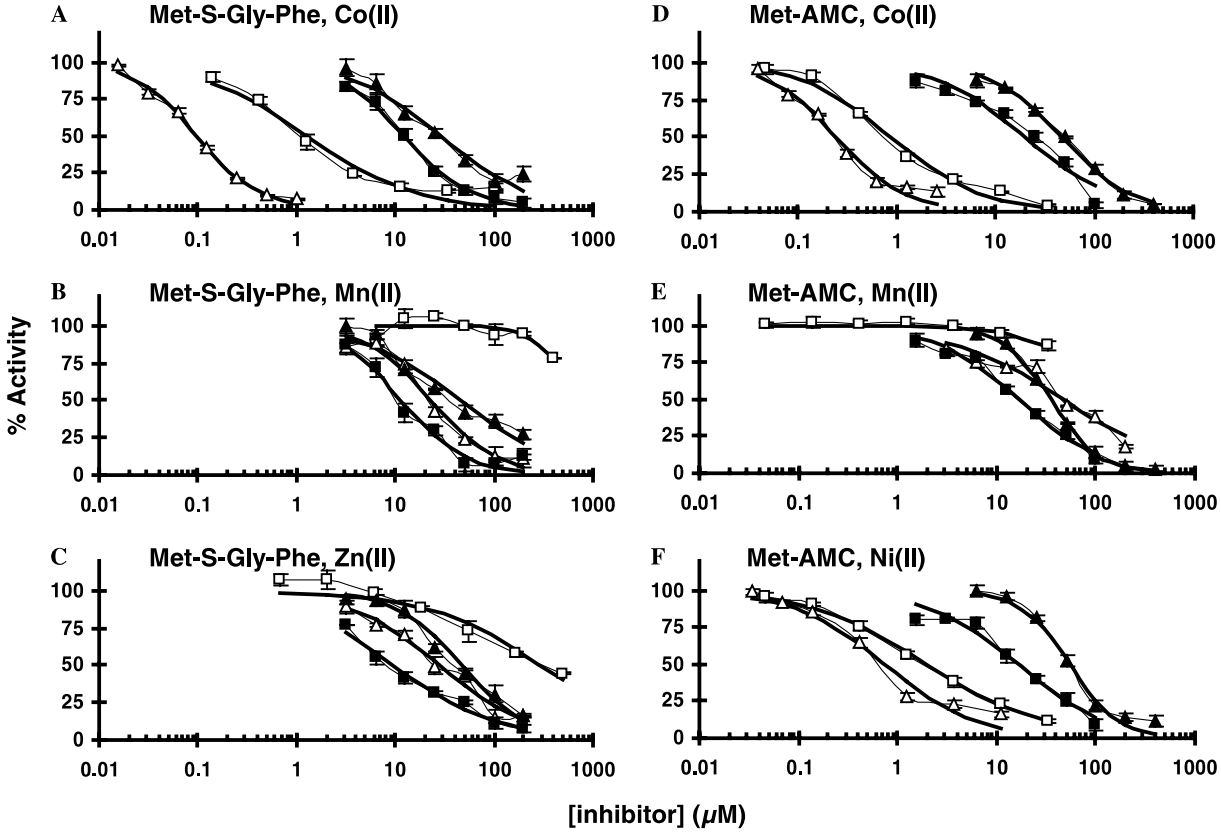

Fig. 4. Inhibition of *Ec*MetAP1 in the colorimetric assay with Met–*S*–Gly–Phe as the substrate (A–C) or in the fluorescence assay with Met-AMC as the substrate (D, E, F) in the presence of Co(II), Mn(II), Zn(II), or Ni(II). Inhibitors are **1** (open squares), **5** (open triangles), **6** (filled squares), and **8** (filled triangles). In the colorimetric assay, mixture contained 200 nM apo-*Ec*MetAP1, 100 μM Met–*S*–Gly–Phe, and a divalent metal (20 μM $CoCl_2$, 20 μM $MnCl_2$, or 200 nM $ZnCl_2$). In the fluorescence assay, the mixture contained 1 μM apo-*Ec*MetAP1, 400 μM Met-AMC, and a divalent metal (100 μM $CoCl_2$, 100 μM $MnCl_2$, or 10 μM $NiCl_2$).

Table 2
Inhibition of the metal-substituted *Ec*MetAP1s

Compound	IC_{50} (μM)			
	Co-*Ec*MetAP1[a]	Mn-*Ec*MetAP1[a]	Zn-*Ec*MetAP1[a]	Ni-*Ec*MetAP1[b]
1	1.3 ± 0.1	>200	>200	1.9 ± 0.3
2	0.21 ± 0.02	>200	>200	0.21 ± 0.05
3	37.0 ± 2.0	>200	>200	5.1 ± 0.9
4	39.9 ± 4.0	>200	>200	13.1 ± 2.2
5	0.10 ± 0.01	23.3 ± 3.4	22.4 ± 4.2	0.76 ± 0.07
6	12.3 ± 1.5	11.5 ± 1.1	9.3 ± 1.7	22.3 ± 2.3
7	22.9 ± 2.4	25.2 ± 2.3	16.7 ± 1.5	12.5 ± 1.1
8	28.6 ± 3.7	44.3 ± 5.7	49.8 ± 1.5	35.7 ± 0.1
9	29.6 ± 0.9	44.1 ± 1.8	36.5 ± 4.7	ND[c]

[a] The IC_{50} values were determined in a continuous colorimetric assay (Met–*S*–Gly–Phe) with 200 nM apo-*Ec*MetAP1 and a divalent metal (20 μM $CoCl_2$, 20 μM $MnCl_2$, or 200 nM $ZnCl_2$).

[b] The IC_{50} values were determined in a continuous fluorescence assay (Met-AMC) with 1 μM apo-*Ec*MetAP1 and 10 μM $NiCl_2$.

[c] ND: not determined.

and Ni(II) for *Sc*MetAP1 [13]. For a given enzyme, there were discrepancies as to which divalent metal could activate it. Our results showed that the Met–*S*–Gly–Phe assay could detect activation by Zn(II) but not by Ni(II), and, on the other hand, the Met-AMC assay is more sensitive to Ni(II) activation but not to Zn(II) activation. A likely scenario is that both Ni(II) and Zn(II) could incorporate into the enzyme active site and form the necessary assembly for catalysis, but because of the different substrate specificities of the different metal-substituted enzymes, the metal activation may be detectable by one substrate but not by the other.

The occupation by different metals may cause subtle changes at the active site and cause the change of specificity for substrates, as well as specificity for inhibitors. Examples of structural changes upon metal substitution are abundant. The recently solved X-ray structures of copper amino oxidase with Cu(II) replaced by Co(II) and Ni(II) revealed changes in the metal coordination environment [22]. X-ray structures of metal-substituted thermolysin with the catalytic Zn(II) replaced by Co(II), Cd(II), or Mn(II) also explained the altered activities by changes in metal coordination geometry and conformational changes that disrupt the active site to varying degrees [23]. A structure of Mn-*Ec*MetAP1 or other metal-substituted *Ec*MetAP1s, in comparison with the structure of Co-*Ec*MetAP1, would provide the valuable information on the metal site and shed light on the substrate and inhibitor specificity among the metal-substituted *Ec*MetAP1s.

Recent data suggest that the MetAPs in its native state inside cells may have a different metal other than Co(II) used often in in vitro studies. The most possible candidates for the in vivo metal are Fe(II), Zn(II), and Mn(II). Holz and co-workers [15–17] have provided evidences for Fe-*Ec*MetAP1 and Fe-*Pf*MetAP2 under an anaerobic condition and further suggested only one metal ion at the active site for maximal activity. Zn(II) was abundant in cells expressing *Ec*MetAP1 [15], and Walkers and Badshaw [13] showed that Zn(II) stimulated *Sc*MetAP1 activity in the presence of glutathione while Co-*Sc*MetAP1 lost activity when glutathione is presented. Mn(II) is also a viable candidate, since the Mn(II) loaded MetAP is catalytically competent (this study and [21]), and aminopeptidase P (APP), an enzyme that shares the same "pita bread" structural fold with MetAPs and has identical conserved metal ligands, uses Mn(II) at its active site [24,25]. The X-ray structure of *E. coli* aminopeptidase P had two Mn(II) ions at its dinuclear metal site [26]. Both Fe(II) and Mn(II) were elevated to higher concentrations while Zn(II) was abundant and Co(II) was undetectable before and after the overexpression [15]. At the time when the in vivo metal has not been defined, it is important to study the properties of *Ec*MetAP1 with metal substitution and decipher the specificity of these enzymes for substrates and inhibitors.

Antiangiogenic fumagillin from nature and their analogues are potent inhibitors for *Hs*MetAP2 [8,9]. However, few inhibitors for bacterial and fungal MetAPs have been reported. From a small scale random screening, we have identified several Co-*Ec*MetAP1 inhibitors with novel structures. They are competitive inhibitors, and their synthetic derivatives improved the inhibitory potencies from micromolar in the leads to 100 nM on Co-*Ec*MetAP1 [19].

However, these and other Co(II)-*Ec*MetAP1 inhibitors could be useful as drug leads only if the in vivo metal is Co(II) or if they can also inhibit MetAPs with an in vivo metal at their active site. At this time when the in vivo metal is still to be defined, these inhibitors would be, at least, excellent probes for the active site of metal-substituted MetAPs. The inhibitors from random screening inhibited Co- and Ni-EcMetAP1s but could not inhibit Zn- or Mn-*Ec*MetAP1, while AHHpA (**6**) and other substrate-like inhibitors (**7**–**9**) inhibited Co-, Mn-, Zn-, and Ni-*Ec*MetAP1s. There were clear indications of change of specificity for inhibitors, depending on the divalent metal occupying the active site. The inhibitors tested represent only a limited number of structural types, and we are in the process of finding the inhibitors for the metal-substituted MetAPs and elucidating the structural requirements in inhibiting these enzymes.

References

[1] R.A. Bradshaw, W.W. Brickey, K.W. Walker, N-terminal processing: the methionine aminopeptidase and *N* alpha-acetyl transferase families, Trends Biochem. Sci. 23 (1998) 263–267.

[2] W.T. Lowther, B.W. Matthews, Structure and function of the methionine aminopeptidases, Biochim. Biophys. Acta 1477 (2000) 157–167.

[3] N.T. Perna, G. Plunkett, V. Burland, B. Mau, J.D. Glasner, D.J. Rose, G.F. Mayhew, P.S. Evans, J. Gregor, H.A. Kirkpatrick, G. Posfai, J. Hackett, S. Klink, A. Boutin, Y. Shao, L. Miller, E.J. Grotbeck, N.W. Davis, A. Lim, E.T. Dimalanta, K.D. Potamousis, J. Apodaca, T.S. Anantharaman, J. Lin, G. Yen, D.C. Schwartz, R.A. Welch, F.R. Blattner, Genome sequence of enterohaemorrhagic *Escherichia coli* O157:H7, Nature 409 (2001) 529–533.

[4] S.Y. Chang, E.C. McGary, S. Chang, Methionine aminopeptidase gene of *Escherichia coli* is essential for cell growth, J. Bacteriol. 171 (1989) 4071–4072.

[5] C.G. Miller, A.M. Kukral, J.L. Miller, N.R. Movva, pepM is an essential gene in *Salmonella typhimurium*, J. Bacteriol. 171 (1989) 5215–5217.

[6] X. Li, Y.H. Chang, Amino-terminal protein processing in *Saccharomyces cerevisiae* is an essential function that requires two distinct methionine aminopeptidases, Proc. Natl. Acad. Sci. USA 92 (1995) 12357–12361.

[7] M.D. Vaughan, P.B. Sampson, J.F. Honek, Methionine in and out of proteins: targets for drug design, Curr. Med. Chem. 9 (2002) 385–409.

[8] E.C. Griffith, Z. Su, S. Niwayama, C.A. Ramsay, Y.H. Chang, J.O. Liu, Molecular recognition of angiogenesis inhibitors fumagillin and ovalicin by methionine aminopeptidase 2, Proc. Natl. Acad. Sci. USA 95 (1998) 15183–15188.

[9] N. Sin, L. Meng, M.Q. Wang, J.J. Wen, W.G. Bornmann, C.M. Crews, The anti-angiogenic agent fumagillin covalently binds and inhibits the methionine aminopeptidase, MetAP-2, Proc. Natl. Acad. Sci. USA 94 (1997) 6099–6103.

[10] S. Liu, J. Widom, C.W. Kemp, C.M. Crews, J. Clardy, Structure of human methionine aminopeptidase-2 complexed with fumagillin, Science 282 (1998) 1324–1327.

[11] W.T. Lowther, A.M. Orville, D.T. Madden, S. Lim, D.H. Rich, B.W. Matthews, *Escherichia coli* methionine aminopeptidase: implications of crystallographic analyses of the native, mutant, and inhibited enzymes for the mechanism of catalysis, Biochemistry 38 (1999) 7678–7688.

[12] T.H. Tahirov, H. Oki, T. Tsukihara, K. Ogasahara, K. Yutani, K. Ogata, Y. Izu, S. Tsunasawa, I. Kato, Crystal structure of methionine aminopeptidase from hyperthermophile, *Pyrococcus furiosus*, J. Mol. Biol. 284 (1998) 101–124.

[13] K.W. Walker, R.A. Bradshaw, Yeast methionine aminopeptidase I can utilize either Zn^{2+} or Co^{2+} as a cofactor: a case of mistaken identity?, Protein Sci. 7 (1998) 2684–2687.

[14] G. Yang, R.B. Kirkpatrick, T. Ho, G.F. Zhang, P.H. Liang, K.O. Johanson, D.J. Casper, M.L. Doyle, J.P. Marino, S.K. Thompson, W. Chen, D.G. Tew, T.D. Meek, Steady-state kinetic characterization of substrates and metal ion specificities of the full-length and N-terminally truncated recombinant human methionine aminopeptidases (type 2), Biochemistry 40 (2001) 10645–10654.

[15] V.M. D'souza, R.C. Holz, The methionyl aminopeptidase from *Escherichia coli* can function as an iron(II) enzyme, Biochemistry 38 (1999) 11079–11085.

[16] V.M. D'souza, B. Bennet, A.J. Copik, R.C. Holz, Divalent metal binding properties of the methionyl aminopeptidase from *Escherichia coli*, Biochemistry 39 (2000) 3817–3826.

[17] L. Meng, S. Ruebush, V.M. D'souza, A.J. Copik, S. Tsunasawa, R.C. Holz, Overexpression and divalent metal binding properties of the methionyl aminopeptidase from *Pyrococcus furiosus*, Biochemistry 41 (2002) 7199–7208.

[18] Y. Zhou, X.C. Guo, T. Yi, T. Yoshimoto, D. Pei, Two continuous spectrophotometric assays for methionine aminopeptidase, Anal. Biochem. 280 (2000) 159–165.

[19] Q.L. Luo, J.Y. Li, Z.Y. Liu, L.L. Chen, J. Li, Z. Qian, Q. Shen, Y. Li, G.H. Livingston, Q.Z. Ye, F.J. Nan, Discovery and structural modification of inhibitors of methionine aminopeptidases from *Escherichia coli* and *Saccharomyces cerevisiae*, J. Med. Chem. (2003) 2631–2640.

[20] S.J. Keding, N.A. Dales, S. Lim, D. Beauliu, D.H. Rich, Synthesis of (3*R*)-amino-(2*S*)-hydroxy amino acids for inhibition of methionine aminopeptidase-1, Synth. Commun. 28 (1998) 4463–4470.

[21] V.M. D'souza, S.I. Swierczek, N.J. Cosper, L. Meng, S. Ruebush, A.J. Copik, R.A. Scott, R.C. Holz, Kinetic and structural characterization of manganese(II)-loaded methionyl aminopeptidases, Biochemistry 41 (2002) 13096–13105.

[22] S. Kishishita, T. Okajima, M. Kim, H. Yamaguchi, S. Hirota, S. Suzuki, S. Kuroda, K. Tanizawa, M. Mure, Role of copper ion in bacterial copper amine oxidase: spectroscopic and crystallographic studies of metal-substituted enzymes, J. Am. Chem. Soc. 125 (2003) 1041–1055.

[23] D.R. Holland, A.C. Hausrath, D. Juers, B.W. Matthews, Structural analysis of zinc substitutions in the active site of thermolysin, Protein Sci. 4 (1995) 1955–1965.

[24] G.S. Cottrell, N.M. Hooper, A.J. Turner, Cloning, expression, and characterization of human cytosolic aminopeptidase P: a single manganese(II)-dependent enzyme, Biochemistry 39 (2000) 15121–15128.

[25] W.T. Lowther, B.W. Matthews, Metalloaminopeptidases: common functional themes in disparate structural surroundings, Chem. Rev. 102 (2002) 4581–4607.

[26] M.C. Wilce, C.S. Bond, N.E. Dixon, H.C. Freeman, J.M. Guss, P.E. Lilley, J.A. Wilce, Structure and mechanism of a proline-specific aminopeptidase from *Escherichia coli*, Proc. Natl. Acad. Sci. USA 95 (1998) 3472–3477.